The Role of Large-Scale Motions in Catalysis by Dihydrofolate Reductase

E. Joel Loveridge,[†,‖] Lai-Hock Tey,[†,⊥] Enas M. Behiry,[†] William M. Dawson,[†] Rhiannon M. Evans,[†,#] Sara B.-M. Whittaker,[‡] Ulrich L. Günther,[‡] Christopher Williams,[§] Matthew P. Crump,[§] and Rudolf K. Allemann[*,†]

[†]School of Chemistry, Cardiff University, Park Place, Cardiff CF10 3AT, United Kingdom
[‡]HWB-NMR, School of Cancer Studies, University of Birmingham, Vincent Drive, Birmingham B15 2TT, United Kingdom
[§]School of Chemistry, University of Bristol, Cantocks Close, Bristol BS8 1TS, United Kingdom

S *Supporting Information*

ABSTRACT: Dihydrofolate reductase has long been used as a model system to study the coupling of protein motions to enzymatic hydride transfer. By studying environmental effects on hydride transfer in dihydrofolate reductase (DHFR) from the cold-adapted bacterium *Moritella profunda* (MpDHFR) and comparing the flexibility of this enzyme to that of DHFR from *Escherichia coli* (EcDHFR), we demonstrate that factors that affect large-scale (i.e., long-range, but not necessarily large amplitude) protein motions have no effect on the kinetic isotope effect on hydride transfer or its temperature dependence, although the rates of

the catalyzed reaction are affected. Hydrogen/deuterium exchange studies by NMR-spectroscopy show that MpDHFR is a more flexible enzyme than EcDHFR. NMR experiments with EcDHFR in the presence of cosolvents suggest differences in the conformational ensemble of the enzyme. The fact that enzymes from different environmental niches and with different flexibilities display the same behavior of the kinetic isotope effect on hydride transfer strongly suggests that, while protein motions are important to generate the reaction ready conformation, an optimal conformation with the correct electrostatics and geometry for the reaction to occur, they do not influence the nature of the chemical step itself; large-scale motions do not couple directly to hydride transfer proper in DHFR.
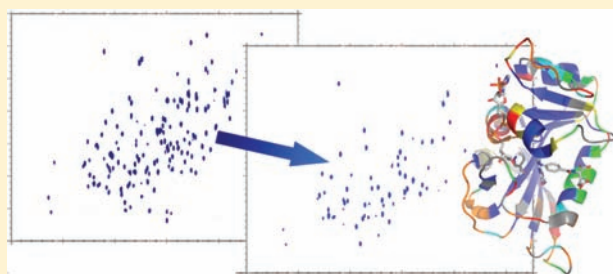
INTRODUCTION

The role played by protein motions in driving the chemical step of an enzyme-catalyzed reaction is the subject of vigorous debate.[1−8] Such promoting motions are distinct from motions associated with the physical steps during enzyme catalysis such as substrate binding, product release, or other conformational changes, which are well described in terms of millisecond—second (ms—s) time scale dynamics. It has been suggested that enzyme dynamics and flexibility are important not just for the physical events but also for the chemical step itself.[5−7,9,10] The potential involvement of protein motions in driving the chemistry of enzyme catalyzed reactions is often studied for hydrogen transfer, where quantum mechanical tunnelling plays a role and the width of the reaction barrier is as important in determining the reaction rate as its height. An 'environmentally coupled tunnelling' model has been proposed to explain unusual kinetic behavior of enzymatic H-transfer reactions.[7,11] In this model, slower (μs—ms) protein motions such as large-scale loop or subdomain movements as well as active site remodelling promote the reaction by creating wavefunction degeneracy in a reaction ready conformation (RRC), while faster (fs—ns) short-range motions can reduce the reaction barrier in the RRC. The temperature dependence of the primary hydrogen kinetic isotope

effect has been used as the major indicator of the nature of the coupling of these motions to the reaction coordinate. Therefore, changes to the coupling of protein motions to the reaction are expected to alter the kinetic isotope effects and their temperature dependences.[7,11] However, several experimental observations[12−16] and results based on computation[3,17,18] have suggested inconsistencies with this model.

Changing the composition of the solvent will have a number of effects on the enzyme and its catalyzed reaction. Increasing the viscosity will reduce the rate of diffusion through the medium and therefore slow ligand binding as well as motions within the protein itself. Reducing the dielectric constant (i.e., reducing the polarity of the medium) will reduce the shielding effect of the medium on dipole—dipole interactions. This will strengthen electrostatic interactions in the transition state and so directly alter the reaction barrier, as well as altering the flexibility of the protein spanning hydrogen-bonding network.[19] The coupling of protein motions to the reaction coordinate can therefore be tested experimentally through changes of the solvent composition.

Dihydrofolate reductase (DHFR) catalyzes the reduction of 7,8-dihydrofolate to 5,6,7,8-tetrahydrofolate using reduced nicotinamide adenine dinucleotide phosphate (NADPH) as a cofactor. DHFRs from organisms living at high and moderate temperatures have been studied extensively with the goal of understanding the relationship between enzyme structure, protein dynamics, and chemical catalysis.[1,2,6,20,21] The experimentally accessible temperature range has been extended in studies of the structural and kinetic adaptation of the DHFR from the hyperthermophile *Thermotoga maritima* (TmDHFR)[12,22−24] and more recently from the baro- and psychrophilic bacterium *Moritella profunda* (MpDHFR), isolated from sediments 2.8 km below the surface of the Atlantic Ocean.[25−29] The tertiary structure of MpDHFR is similar to that of DHFR from *Escherichia coli* (EcDHFR) and no obvious structural indications of adaptation to high pressure and low temperature have been found.[27] Detailed structural and kinetic studies of a number of DHFRs from related *Moritella* species and from other deep-sea bacteria did not reveal any specific evidence of pressure adaptation.[30,31]

We have previously reported the effect of temperature and pH in the steady state of the MpDHFR catalyzed reaction,[29] where physical processes rather than the actual chemical step limit the reaction rate at physiological pH as is also the case for EcDHFR.[32] Here we provide insight into the role of protein motions in DHFR catalysis from measurements of the effects of temperature, pH, and solvent composition on the chemical step during MpDHFR catalysis and of hydrogen/deuterium exchange rates in MpDHFR and EcDHFR by NMR spectroscopy. Hydrogen/deuterium exchange provides a measure of solvent accessibility and is therefore a measure of the flexibility of the protein on a slow (by NMR) time scale and of the shielding effects of secondary structural elements and ligands.[33,34] Our results indicate the importance of protein dynamics for the generation of the RRC on the free-energy landscape, but suggest that the chemical step itself is not promoted significantly by motions during catalysis by DHFR.

■ MATERIALS AND METHODS

Chemicals. NADPH was purchased from Melford. Dihydrofolate was prepared by dithionite reduction of folate.[35] 4-(*R*)-NADPD was prepared as described previously,[36] as was recombinant MpDHFR.[27] 4-(*S*)-NADPD was prepared in the same way as 4-(*R*)-NADPD, except that glucose-1-D (Cambridge Isotope Laboratories) was used as the deuterium source and glucose dehydrogenase from *Pseudomonas* sp. (Sigma) was the enzyme. The concentrations of NADPH/NADPD and H_2F were determined spectrophotometrically using extinction coefficients of 6200 cm^{-1} M^{-1} at 339 nm and 28 000 cm^{-1} M^{-1} at 282 nm, respectively.[37] Where applicable, solutions containing 17%, 33%, and 50% cosolvent (volume cosolvent per final solution volume) were used. The pH was adjusted after the addition of cosolvent to ensure consistency. Details of dielectric constants and viscosities of solvent mixtures have been reported previously.[14]

Circular Dichroism Spectroscopy. Circular dichroism (CD) experiments were performed on an Applied Photophysics Chirascan spectrophotometer using 2.5 μM protein in 5 mM potassium phosphate buffer (pH 7.0) containing the desired cosolvent where appropriate. Spectra were measured between 195 and 400 nm in quartz cuvettes (0.1 cm path length, Helma) under N_2. Mean residue ellipticities $[\Theta]_{MRE}$ were calculated using the equation $[\Theta]_{MRE} = \Theta/(10ncl)$, where Θ is the measured ellipticity in mdeg, n is the number of backbone amide bonds, c is the concentration of protein in mol L^{-1}, and l is the path length in cm. Thermal denaturation experiments were performed using temperature steps of 1 °C between 20 and 70 °C, with 1 min equilibration at the

desired temperature prior to measurement. Melting temperatures were determined by plotting $[\Theta]_{MRE}$ at 222 nm against temperature.

Steady-State Kinetic Measurements. Turnover rates were measured spectrophotometrically on a JASCO V-660 spectrophotometer by following the decrease in absorbance at 340 nm during the reaction (ε_{340} (NADPH + H_2F) = 11 800 M^{-1} cm^{-1}).[38] Rates were determined at pH 7 using 20 nM enzyme in 100 mM potassium phosphate containing 100 mM NaCl and 10 mM β-mercaptoethanol, and at pH 9 using 50 nM enzyme in MTEN buffer (50 mM morpholinoethanesulfonic acid, 25 mM Tris, 25 mM ethanolamine, 100 mM NaCl, and 10 mM β-mercaptoethanol). The enzyme was preincubated at the desired temperature with NADPH (0.1−200 μM) for 1 min to avoid hysteresis[32] prior to addition of H_2F (100 μM). Each data point is the result of three independent measurements. At low NADPH concentrations in certain cosolvents, the errors on the measured rates were relatively high and it was therefore not possible to measure accurate K_m values.

Pre-Steady-State Kinetic Measurements. Hydride transfer rates were measured under single-turnover conditions on an Applied Photophysics stopped-flow spectrophotometer. The enzyme (20 μM final concentration) was preincubated with NADPH (8 μM final concentration) for at least 5 min in 100 mM potassium phosphate (pH 7.0) containing 100 mM NaCl and 10 mM β-mercaptoethanol and the reaction started by rapidly mixing with H_2F (200 μM final concentration) in the same buffer. Reduction of the fluorescence resonance energy transfer from the enzyme to NADPH during the reaction was observed by exciting the sample at 292 nm and measuring the emission using a 400 nm cutoff output filter. All experiments were repeated at least nine times. Varying the concentrations of the reagents showed that the measured rates were limiting rates for hydride transfer, regardless of solvent composition.

Hydrogen/Deuterium Exchange Measurements. Rates of H/D exchange (HDX) at 20 °C were determined by NMR on a Varian INOVA 900 MHz (^{1}H) spectrometer equipped with a cryogenically cooled HCN probe. Proteins for NMR experiments were purified by anion exchange on Q-sepharose resin followed by gel filtration on a prep grade Superdex 75 column. This ensures that no folate is present in the apoenzyme prior to NMR measurements, which would be the case using our usual purification method.[27] EcDHFR and MpDHFR, as the apoenzyme and the NADP$^+$/folate complexes (6-fold excess of ligands), were prepared as 2 mM stocks in 50 mM potassium phosphate buffer, pH 7, containing 1 mM NaCl, 10 mM β-mercaptoethanol, and 10% D_2O. As MpDHFR cannot be freeze-dried without substantial loss of activity, HDX experiments were performed by dilution rather than resuspension. The concentrated stock was diluted 10-fold into H_2O and D_2O 24 h prior to measurement to create 'before' and 'after' samples, which were used to optimize the acquisition parameters and to obtain optimized shim maps for HDX experiments. HDX was then performed by diluting the concentrated stock 10-fold into D_2O immediately prior to insertion into the magnet. The time between sample mixing and acquisition of the first spectrum was recorded. SOFAST-HMQC spectra[39] were recorded at regular intervals until no further exchange was seen, increasing the number of scans with time to maximize signal (see Supporting Information for full details). Spectra were processed using NMRPipe[40] and analyzed using Analysis 2.1.5 for Linux.[41] Peak intensity (adjusted for changes to the number of scans by dividing by the square root of the ratio of number of scans) was plotted against exchange time (from sample mixing to the midpoint of the spectrum acquisition) and rate constants determined using SigmaPlot 10.

^{1}H−^{15}N crosspeaks for the EcDHFR/NADP$^+$/folate complex were assigned using published data,[42] and connectivity was confirmed using a 3D ^{1}H−^{15}N NOESY-HSQC spectrum acquired on a Varian INOVA 600 MHz (^{1}H) spectrometer equipped with a HCN probe, using 2.4 mM EcDHFR with 15 mM ligands in 50 mM potassium phosphate
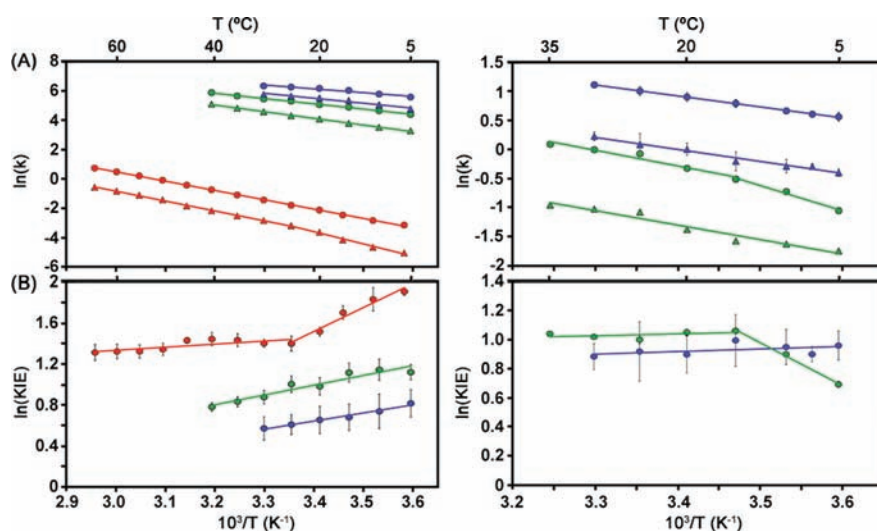
Figure 1. Arrhenius plots (A) for hydride (circles) and deuteride (triangles) transfer and the corresponding KIEs (B) plotted on a logarithmic scale against the inverse temperature for MpDHFR (blue), EcDHFR[37] (green), and TmDHFR[22] (red) catalysis, measured under single turnover conditions at pH 7 (left) and in the steady state at pH 9 (MpDHFR) or 9.5 (EcDHFR)[37] (right).

Table 1. Activation Parameters and Corresponding k_H for Hydride Transfer Catalyzed by MpDHFR, EcDHFR and TmDHFR at pH 7

parameter	MpDHFR	EcDHFR[36]	TmDHFR[22]
k_H/s^{-1} [a]	526.8 ± 23.2	203.7 ± 7.4	0.169 ± 0.002
KIE[a]	1.83 ± 0.10	2.71 ± 0.22	4.02 ± 0.29
E_a^H/kJ mol^{-1}	21.6 ± 2.2	29.9 ± 0.6	53.6 ± 0.4[b]
E_a^D/kJ mol^{-1}	28.1 ± 2.6	37.8 ± 0.6	56.0 ± 0.8[b]
ΔE_a/kJ mol^{-1}	6.6 ± 3.4	7.9 ± 0.9	2.5 ± 1.0[b]
$A_H/10^6$ s^{-1}	3.2 ± 0.2	34 ± 5	410 ± 70[b]
$A_D/10^6$ s^{-1}	24 ± 2	320 ± 10	270 ± 90[b]
A_H/A_D	0.13 ± 0.09	0.11 ± 0.02	1.54 ± 0.36[b]
$\Delta H^{\ddagger}_H$/kJ mol^{-1}	19.2 ± 2.2	27.4 ± 0.6	50.9 ± 0.5[b]
$\Delta H^{\ddagger}_D$/kJ mol^{-1}	25.7 ± 2.6	35.3 ± 0.6	53.4 ± 0.8[b]
$\Delta S^{\ddagger}_H$/J mol^{-1}	−128.6 ± 1.4	−109.0 ± 2.5	−88.9 ± 1.2[b]
$\Delta S^{\ddagger}_D$/J mol^{-1}	−111.6 ± 1.2	−90.3 ± 1.8	−92.4 ± 2.3[b]
$\Delta G^{\ddagger}_H$/kJ mol^{-1} [a]	57.5 ± 2.2	59.9 ± 0.6	77.4 ± 0.5
$\Delta G^{\ddagger}_D$/kJ mol^{-1} [a]	59.0 ± 2.6	62.2 ± 0.6	80.9 ± 0.8

[a] At 25 °C. [b] Above 25 °C.

buffer, pH 7, containing 1 mM NaCl, 10 mM β-mercaptoethanol, and 10% D$_2$O. Crosspeaks for apo-EcDHFR were assigned by titration to form the NADP$^+$/folate complex and using a 3D ^{1}H−^{15}N HSQC-NOESY spectrum acquired on a Bruker Avance II+ 700 MHz (^{1}H) spectrometer equipped with a cryogenically cooled HCN probe, using 2.2 mM apo-EcDHFR in the same buffer. Crosspeaks for the MpDHFR/NADP$^+$/folate complex were assigned using standard triple-resonance methods.[43] As all apo-MpDHFR crosspeaks exchanged fully within the dead time of the experiment, no assignment was performed.

^{1}H−^{15}N HSQC spectra were also acquired for the EcDHFR/NADP$^+$/folate complex in the presence of 17, 33, and 50% methanol and glycerol. Spectra were acquired on a Varian INOVA 600 MHz (^{1}H) spectrometer equipped with a HCN probe, using 240 μM EcDHFR with 1.5 mM ligands in 50 mM potassium phosphate buffer, pH 7, containing 1 mM NaCl, 10 mM β-mercaptoethanol, and 10% D$_2$O.

■ RESULTS AND DISCUSSION

Hydride Transfer. The rate constants for hydride transfer (k_H) during MpDHFR catalysis were determined under single

turnover conditions that isolate the chemical step of the reaction cycle.[36] At pH 7, k_H was considerably greater than k_{cat} at all temperatures, as expected from the earlier observation that the primary hydrogen kinetic isotope effect (KIE) in the steady state is unity.[29] At 25 °C, k_H for the MpDHFR-catalyzed reaction was over twice that of the EcDHFR-catalyzed reaction and more than 2 orders of magnitude greater than that of the TmDHFR-catalyzed reaction (Figure 1 and Table 1). The primary hydrogen KIE on MpDHFR-catalyzed hydride transfer was temperature dependent with ΔE_a of 6.6 ± 3.4 kJ mol^{-1}. The primary hydrogen KIE was also determined under steady-state conditions at pH 9 (Figure 1 and Supporting Information), where hydride transfer is rate limiting.[29] Here, the KIE was almost temperature independent with ΔE_a of 1.5 ± 1.1 kJ mol^{-1}. For EcDHFR at elevated pH, the KIE falls below 15 °C due to a partial change in the rate-limiting step.[37] For MpDHFR, a similar fall in the KIE was observed below 5 °C, to 1.98 ± 0.13 at 1 °C (not shown). α-Secondary hydrogen KIEs on MpDHFR and EcDHFR catalysis
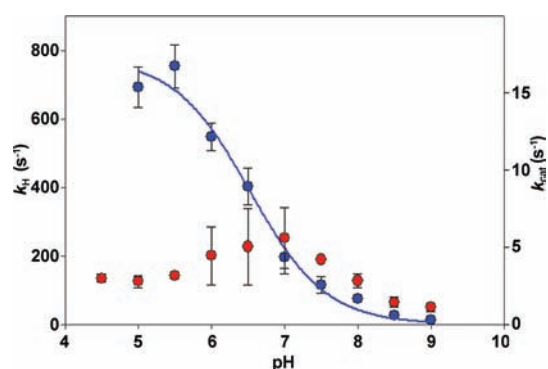
Figure 2. Plots of k_H (blue; left abscissa) and k_{cat} (red; right abscissa)[29] against the pH value of the solution for the MpDHFR catalyzed reaction in MTEN buffer at 5 °C.

were determined under single turnover conditions at pH 7 (Supporting Information). The α-secondary KIEs for both enzymes were temperature independent with average observed values of 1.065 ± 0.022 for EcDHFR and 1.044 ± 0.011 for MpDHFR.

The hydride transfer rate constant for MpDHFR catalysis was dependent on pH with an apparent pK_a of 6.53 ± 0.12 at 5 °C (Figure 2 and Supporting Information). At higher temperatures, the rate constant for the reaction below pH 6 was too high to determine accurately by stopped flow kinetic measurements. The sigmoidal curve observed for hydride transfer is in contrast to the steady state rate constant, which showed a bell shaped pH dependence demonstrating that the reduction in the steady-state rate constant for MpDHFR at low pH is not due to enzyme inactivation.[29] The rate constants for MpDHFR-catalyzed hydride and deuteride transfer were also measured in D_2O (Supporting Information). A considerable increase in both rate constants was seen, leading to an apparent inverse solvent KIE. However, measurement of k_H at varying values of pD in D_2O demonstrated that this was the consequence of a D_2O-induced shift of the apparent pK_a (to 7.13 ± 0.13, a shift of 0.60 ± 0.03 pH units) rather than any intrinsic effect on the reaction.[36,44]

The Effect of Organic Cosolvents. The effect of cosolvents on the secondary structure of MpDHFR was investigated by CD spectroscopy. Some loss of structure was evident from the CD spectra in the presence of ethanol, isopropyl alcohol, and tetrahydrofuran, but little change of the global structure was observed in the presence of glycerol, ethylene glycol, sucrose, and methanol (Supporting Information). NMR spectroscopy in the presence of methanol or glycerol on the other hand revealed local solvent specific changes of the conformation of EcDHFR (vide infra). The addition of 50% glycerol and 30% sucrose increased the melting temperature of MpDHFR from 37.5 ± 0.8 °C[29] to 51.5 ± 0.5 and 47.2 ± 0.9 °C, respectively, while the melting temperature in 50% methanol (35.1 ± 0.4 °C) was similar to that in the absence of cosolvent (Supporting Information). Interestingly, methanol appears to have a less pronounced effect on MpDHFR than it does on EcDHFR; the melting temperature of EcDHFR was reduced from 51 to 26 °C in 50% methanol.[13]

The steady-state rate constant (k_{cat}) at pH 7 and pH 9 and the rate constant for hydride transfer (k_H) at pH 7 were measured at 20 °C for the MpDHFR catalyzed reaction in the presence of organic cosolvents and cosolutes (Figure 3 and Supporting Information). Increasing the concentration of cosolvent/cosolute led
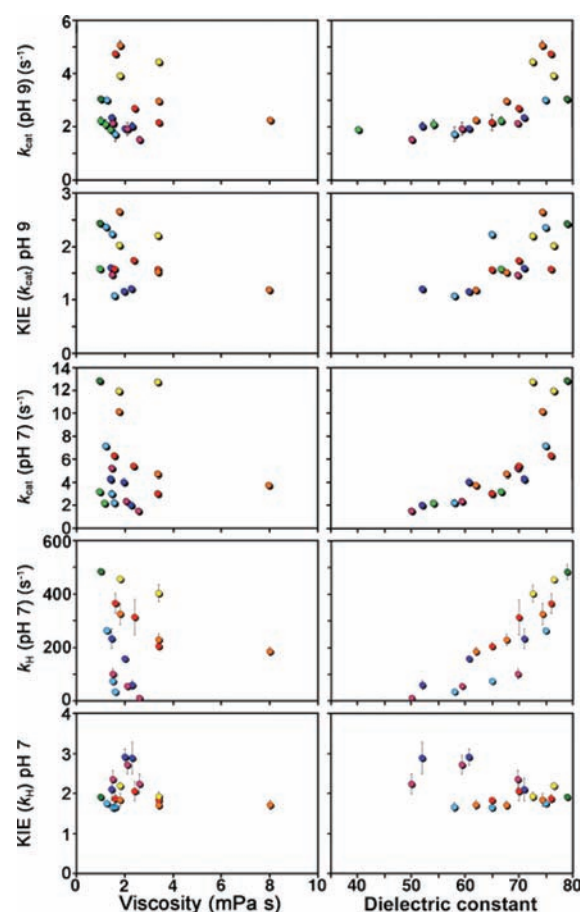

Figure 3. Plots of k_{cat} and KIE on k_{cat} at pH 9, k_{cat} at pH 7, and k_H and KIE on k_H at pH 7 for the MpDHFR-catalyzed reaction against solution viscosity (left) and dielectric constant (right). Colors represent different cosolvents, where dark green denotes no cosolvent, light blue = methanol, dark blue = ethanol, purple = isopropyl alcohol, red = ethylene glycol, orange = glycerol, yellow = sucrose, and light green = tetrahydrofuran. Not all data could be acquired accurately for all cosolvents. Figures for individual cosolvents can be found in Supporting Information.

to a reduction of all three rate constants in a manner proportional to the dielectric constant but not the viscosity of the medium, as seen from the fact that the combined data for all cosolvents form a cluster when plotted against viscosity, whereas a clear overall trend against dielectric constant is visible. The use of multiple cosolvents is important here, as use of only a small number of solvent conditions might lead to the conclusion that a viscosity effect is visible (Supporting Information). However, simultaneous comparison of the data for all cosolvents used here shows that any apparent trend against viscosity with a single cosolvent is in fact due to the general trend against dielectric constant. This can be seen by comparing isoviscous solvent mixtures, which give large differences in rate constant, with isodielectric solvent mixtures, which give far smaller differences in rate constant.

The effect of dielectric constant on the reaction is consistent with electrostatic effects playing the major role in controlling the rate constant for hydride transfer.[3] It is worthy of note that a low dielectric constant should be expected to favor catalysis through electrostatic effects by reducing the shielding of stabilizing electrostatic effects within the active site. This is in apparent contrast to our results, which show catalysis to be favored by a high dielectric
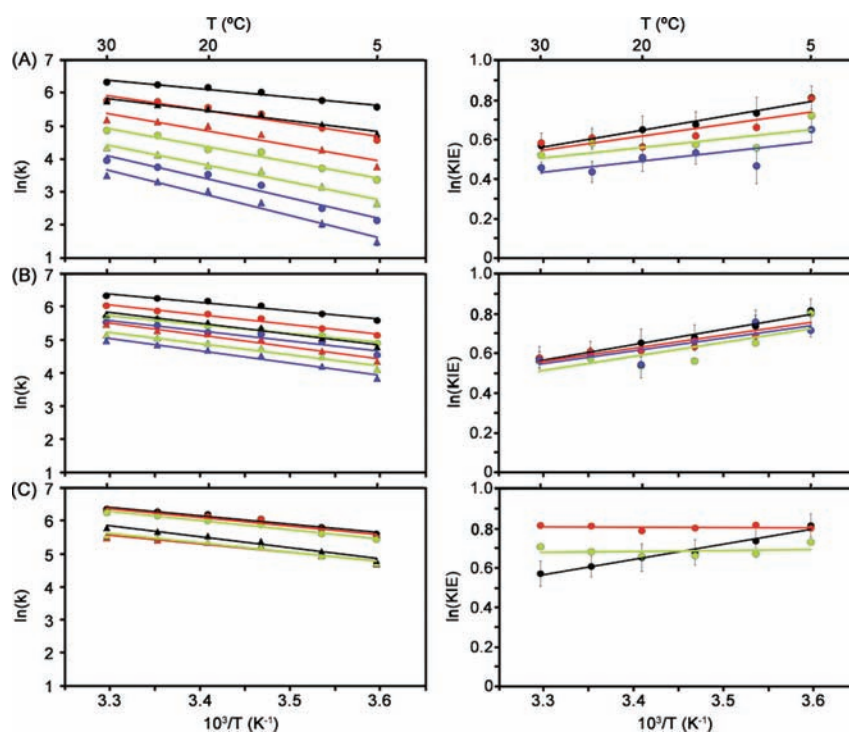
Figure 4. Arrhenius plots for MpDHFR-catalyzed hydride (circles) and deuteride (triangles) transfer (left) and the corresponding KIEs plotted on a logarithmic scale against the inverse temperature (right) at pH 7 in the presence of 0% (black), 17% (red), 33% (green; 30% in the case of sucrose), and 50% (blue) methanol (A), glycerol (B), or sucrose (C).

constant. It is likely that reducing the dielectric constant of the solvent, which in effect reduces the difference between the dielectric constant within the active site and that of the surrounding medium, reduces the protection of the carefully aligned dipoles within the active site from more remote dipoles that may be deleterious to transition state stabilization.

Ivković-Jensen and Kostić's combination of the Eyring equation with the Eaton−Ansari extension of Kramers' theory[45−47] was applied to further evaluate the effect of viscosity on the rate constant, revealing that neither k_{cat} nor k_H correlated with viscosity for any value of internal protein friction (Supporting Information). Furthermore, plotting the normalized $1/k_{cat}$ against the relative viscosity according to the method of Kirsch[48,49] gave poor fits (Supporting Information) strongly indicating that diffusion plays a minor role in limiting the reaction rate. The steady-state data did not indicate reversible inhibition and the values for k_{cat} were unaffected by prolonged incubation of the enzyme with the solvents (data not shown), although the CD data (vide supra) suggest that in isopropyl alcohol and tetrahydrofuran the reduction of the rate constants is partly due to a degree of solvent-induced denaturation.

The KIE on k_H at pH 7 was largely independent of the solvent composition (Figure 3 and Supporting Information), whereas at pH 9, the KIE on k_{cat} decreased as the dielectric constant decreased. This suggests a change in rate-limiting step at pH 9 as the solvent composition is changed showing that solvent composition has a greater influence on the physical steps of the reaction than on the chemical step. K_m values could not be determined accurately in all cases due to high errors on the measured rate data at low cofactor concentrations in certain cosolvents, but in general, the presence of cosolvent reduced the K_m, leading to an initial increase in k_{cat}/K_m followed by a decrease as the cosolvent concentration was increased further (Supporting Information).

The effect of solvent composition on the temperature dependence of the KIE on k_H at pH 7 was also studied (Figure 4 and Supporting Information). Studies of solvent effects on the temperature dependence of the KIE at pH 9 were not performed as the degree to which hydride transfer is rate limiting is changed by the solvent composition (vide supra), making meaningful analysis impossible. At pH 7, neither methanol nor glycerol had a significant effect on the temperature dependence of the primary KIE of the reaction, although methanol caused a significant rise in the activation energy and a reduction in the KIE itself (Supporting Information). The presence of sucrose led to temperature independent KIEs, as had been observed previously for EcDHFR and TmDHFR,[13,14] although these were slightly depressed in 30% sucrose compared to 17% sucrose. It has also been observed that mutations in the dimer interface of TmDHFR can cause the KIE to become entirely temperature independent, suggesting that relatively minor structural alterations remote from the active site may affect the temperature dependence of the KIE.[12] As the concentrations of methanol and glycerol had similar dielectric constants, while the concentrations of glycerol and sucrose used were isoviscous, it appears that bulk solvent properties have no effect on the temperature dependence of the KIE on k_H.

DHFR Catalysis and Thermophilicity. It is clear that the rate constant for hydride transfer by MpDHFR is greater than that of EcDHFR at all values of pH (k_H for EcDHFR is 480.6 ± 15.1 s^{-1} at 10 °C and pH 5,[36] while k_H of MpDHFR is 690.9 ± 59.1 at 5 °C and pH 5), and 2 orders of magnitude greater than that of TmDHFR (0.870 ± 0.004 at 20 °C, pH 5[13]). However, at the typical operating temperatures of the three DHFRs (2 °C for MpDHFR,[50] 37 °C for EcDHFR and 90 °C for TmDHFR[51]) at pH 7, the hydride transfer rate constants were estimated by linear extrapolation from the Arrhenius plots as 255.0 ± 6.4, 317.3 ± 1.6,

and $8.2 \pm 0.1 \text{ s}^{-1}$, respectively. Similarly, the steady-state rate constants[29] under the same conditions are 5.0 ± 1.5, 35.8 ± 2.6, and $4.5 \pm 2.3 \text{ s}^{-1}$. It therefore appears that MpDHFR is in fact a slightly poorer catalyst than EcDHFR at their respective physiological temperatures and is comparable to TmDHFR in the steady state. The activation energy (and enthalpy) for the hydride transfer reaction is most favorable for MpDHFR and least favorable for TmDHFR (Table 1). This is offset by MpDHFR having the least favorable Arrhenius prefactor (and activation entropy), which compensate for one another such that the Gibbs free energies of activation for MpDHFR and EcDHFR are similar. This behavior is comparable to that observed for the activation parameters for the steady-state reactions of MpDHFR and EcDHFR.[29]

The behaviors of the rate constant for hydride transfer and its KIE show a number of similarities between MpDHFR and EcDHFR. The apparent pK_a values of hydride transfer are approximately equal (6.53 ± 0.12 at 5 °C for MpDHFR; 6.59 ± 0.05 at 10 °C for EcDHFR[36]) and higher than that of TmDHFR (5.79 ± 0.04 at 20 °C[13]). Critically, the temperature dependence of the KIE on hydride transfer is similar to that observed for EcDHFR,[37] and quite different to that of TmDHFR (Figure 1B).[22] It has been shown recently that the KIE on hydride transfer in EcDHFR is temperature dependent below pH 8 and temperature independent at or above this pH, demonstrating that the temperature dependent KIEs observed at pH 7 are indeed physiologically relevant, while the temperature independent KIEs observed at elevated pH are not.[36] The lower value observed for the primary and α-secondary hydrogen KIEs on hydride transfer in MpDHFR than in EcDHFR may suggest increased kinetic complexity on the measurements for MpDHFR. We have previously shown that kinetic complexity leads to an underestimate of the temperature dependence of the KIE,[36] which may also explain why the observed ΔE_a is lower for MpDHFR than for EcDHFR. From the data obtained here, it seems reasonable to conclude that monomeric DHFRs have similar kinetic behavior for the hydride transfer step, exemplified by temperature dependent KIEs under physiological conditions, whereas dimeric DHFRs (TmDHFR is the only DHFR shown to be dimeric so far, although it is likely that other DHFRs from the genus *Thermotoga* are also dimeric[12,52]) have different kinetic behavior exemplified by temperature independent KIEs at elevated temperatures.

Hydrogen/Deuterium Exchange Experiments. HDX was followed in NMR experiments to obtain a measure of protein flexibility (Figure 5 and Supporting Information). NMR was chosen over mass spectrometric measurements because it offers single residue resolution. HDX was performed for both the apoenzyme and the DHFR/NADP$^+$/folate ternary complex, which can serve as a model for the DHFR/NADPH/dihydrofolate Michaelis complex.[53,54] The apoenzyme is not affected by shielding effects from the ligands and so yields a clearer picture of the intrinsic flexibility of the protein itself, while the complex more accurately represents the situation during catalysis.

The spectra of both apo-EcDHFR and apo-MpDHFR were of much lower quality than those of the complex with NADP$^+$ and folate. Spectra for the complexes could therefore be acquired considerably faster than for the apoenzyme (Supporting Information). Assignment of the apo-EcDHFR resonances by standard triple-resonance techniques was not attempted due to this low spectral quality. Titration of apo-EcDHFR with a 1:1 mixture of NADP$^+$ and folate revealed that the free and bound states are in slow exchange on the NMR time scale, complicating assignment by that route, although the observed improvement to
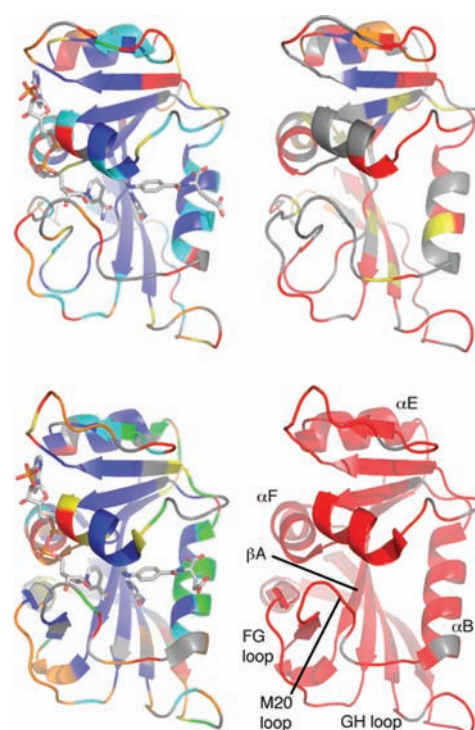

Figure 5. Cartoon representations of EcDHFR (top) and MpDHFR (bottom) as the DHFR/NADP$^+$/folate complexes (left) and as apoenzymes (right) showing half-lives ($t_{1/2}$) of H/D exchange. Gray = no data, blue = no exchange after 24 h, cyan = $t_{1/2} > 30$ min, green = $t_{1/2}$ 10−30 min, yellow = $t_{1/2}$ 2−10 min, orange = $t_{1/2} < 2$ min, and red = $t_{1/2}$ too small to measure. Secondary structural elements discussed in the text are indicated for apo-MpDHFR. Structures are from PDB files 1RX2[53] and 2ZZA.

the spectrum demonstrated that the low spectral quality was intrinsic to the apoenzyme and not due to poor sample quality. Partial assignments ($\sim$70%) were instead obtained using a 3D ^{1}H−^{15}N NOESY-HSQC spectrum to confirm connectivity and residue type as well as by comparison to the assignments of the EcDHFR/NADP$^+$/folate complex. Many residues showed multiple peaks in the ^{1}H−^{15}N HSQC of apo-EcDHFR as has been observed previously,[55] demonstrating conformational heterogeneity.

In general, HDX was much faster for the apoenzymes than for equivalent complexes (Figure 5). The HDX results obtained by NMR are in good agreement with those obtained for apo-EcDHFR in mass spectrometric measurements.[56] For apo-MpDHFR, no significant crosspeaks were visible in the first spectrum after addition of D$_2$O. In contrast, some crosspeaks for apo-EcDHFR showed no exchange after 24 h. These correspond to residues in the central β-sheet of the adenosine-binding domain of the enzyme. MpDHFR is an intrinsically more flexible protein than EcDHFR in that all residues show similar or smaller half-lives of exchange in apo-MpDHFR (Figure 6). The majority of residues that apparently show 'similar' half-lives of exchange simply exchange too quickly for accurate measurement by NMR in both enzymes.

The DHFR/NADP$^+$/folate complexes displayed considerably lower apparent flexibility. In MpDHFR and EcDHFR, significant portions of the secondary structural elements showed no H/D exchange even after 24 h (Figure 5) and the half-lives of exchange were considerably longer in many other cases. This observation is
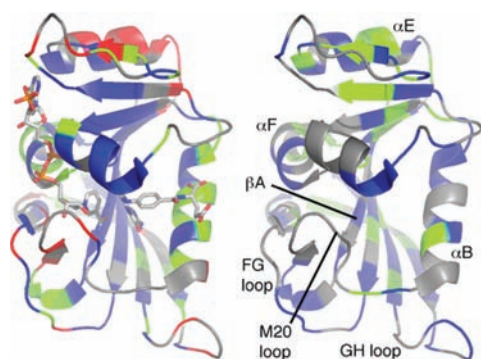
Figure 6. Cartoon representations of MpDHFR as the DHFR/NADP$^+$/folate complex (left) and the apoenzyme (right), comparing half-lives ($t_{1/2}$) of H/D exchange with EcDHFR. Gray = no data, blue = similar $t_{1/2}$, green = $t_{1/2}$ smaller in MpDHFR, red = $t_{1/2}$ smaller in EcDHFR. Secondary structural elements discussed in the text are indicated for the apoenzyme. Figure is drawn from PDB file 2ZZA.

in good agreement with results obtained for EcDHFR using mass spectrometric measurements[57] and with NMR measurements for DHFR from *Lactobacillus casei*.[58] Similarly, it has previously been reported that the melting temperatures of the two enzymes increase upon addition of ligands.[24,29]

Interestingly, and perhaps surprisingly, some residues of the EcDHFR/NADP$^+$/folate complex displayed shorter half-lives of exchange than their counterparts in the MpDHFR/NADP$^+$/folate complex (Figures 5 and 6) suggesting that these regions of EcDHFR may in fact have greater flexibility in the presence of ligands. Notably, these include residues in the M20, FG, and GH loops, all of which are known to be important for the physical progression through the catalytic cycle.[53] In general, these loops have similar solvent exposure in EcDHFR and MpDHFR. However, in EcDHFR, the M20 loop is known to adopt two conformations, closed and occluded, depending on the position within the catalytic cycle,[53] and to fluctuate between these conformations even within the Michaelis complex.[59] On the other hand, Ser 148 of EcDHFR, which is critical for the formation of the occluded conformation, is replaced by Pro 150 in MpDHFR. Replacement of Ser 148 of EcDHFR with Ala is known to prevent the formation of the occluded conformation.[2] It is therefore unlikely that MpDHFR can adopt the occluded conformation. This may lead to reduced flexibility and the observed greater shielding of these loops from solvent despite equal exposure.

Faster H/D exchange in EcDHFR than in MpDHFR is also seen in helix αE and nearby residues (Figure 6), a region of EcDHFR thought to lose structure early in the thermal unfolding process,[60] also suggesting high flexibility, although it should be noted that the residues that show no exchange after 24 h in apo-EcDHFR are also in this region. Apo-DHFR from the thermophile *Geobacillus stearothermophilus* (BsDHFR) has been found to have greater flexibility than EcDHFR at comparable temperatures[61] demonstrating that the general tenet that thermophilic enzymes have reduced and psychrophilic enzymes greater flexibility does not necessarily always apply. It should be noted that binding of methotrexate causes a much larger increase in the melting temperature of MpDHFR than of EcDHFR, suggesting that ligand binding has a greater stabilizing effect on MpDHFR.[24,29] Other active-site regions of the enzyme, notably helices αB and αF, show decreased half-lives of exchange in MpDHFR relative to EcDHFR. These helices are involved in a network of hydrogen

bonds and van der Waals interactions that has been suggested to promote DHFR catalysis;[62] helix αF has also been implicated in the temperature dependence of the KIE in a recent study of BsDHFR.[63] This study also implicates residues in strand βA in the temperature dependence of the KIE, although no exchange in this strand is seen here in either enzyme in the NADP$^+$/folate complex (probably due at least in part to shielding by the ligands) and very little exchange has been seen in βA of BsDHFR below 50 °C.[63] In general, however, the HDX results for the DHFR/NADP$^+$/folate complexes suggest greater flexibility in MpDHFR than in EcDHFR; where EcDHFR shows faster exchange, half-lives were within an order of magnitude of the equivalent MpDHFR values, whereas where MpDHFR showed faster exchange, half-lives were over 2 orders of magnitude smaller than the equivalent EcDHFR values in some cases (Supporting Information). In addition, shielding from the ligands is likely to cause many of the residues to show no exchange, meaning that the flexibility of these residues cannot be determined from the HDX data. Taken together, the HDX results presented here demonstrate greater flexibility of MpDHFR relative to EcDHFR, particularly in active site flanking helices thought to be important for the actual chemical step of catalysis.

NMR of EcDHFR in the Presence of Cosolvents. The effect of cosolvents on EcDHFR (as the DHFR/NADP$^+$/folate complex) was investigated by NMR spectroscopy. On addition of methanol and glycerol, large chemical shift perturbations are seen for certain amide groups, while others show little or no change (Figure 7). The changes in methanol are different to those in glycerol, while the magnitudes and directions of the chemical shift perturbations are residue specific; there is no general solvent effect on the amide chemical shifts. The chemical shift perturbations do not correlate with the surface exposure of the residue, ligand binding, or whether the residue shows chemical exchange (to the excited reactive state) on a microsecond–millisecond time scale in the absence of cosolvent.[54] Most notably, the nonlinearity of some of the chemical shift perturbations with increasing solvent concentrations (see especially G51 and G121 in Figure 7C) demonstrate that the conformational changes caused by the solvent involve a long-lived intermediate rather than simple two-state exchange.[64] Therefore, the presence of organic cosolvent clearly induces slow conformational transitions within the Michaelis complex of EcDHFR. Given that these conformational transitions will be much slower than the chemical step, these data strongly suggest differences in the conformational ensemble of the enzyme in the presence of cosolvents at the point of reaction. Such changes of the conformational ensemble will alter the electrostatics of the enzyme's active site and lead to the observed changes in the rate constants for hydride transfer (vide supra).

The Role of Protein Motions in DHFR Catalysis. The kinetic results obtained here demonstrate that the effect of the addition of cosolvents on the chemical step is the same for MpDHFR, EcDHFR, and TmDHFR, while HDX experiments demonstrate greater flexibility of MpDHFR than EcDHFR. The kinetic results in the presence of cosolvents (vide supra) showed that dielectric constants, but not viscosity, affect the rate constant for hydride transfer; neither parameter affects the primary KIE on hydride transfer or its temperature dependence as has been observed for the EcDHFR[13] and TmDHFR catalyzed reactions.[14] These observations have profound implications for the coupling of protein motions to catalysis.[13] Most notably, the effect of dielectric constant on DHFR catalysis suggests a dominant role for electrostatic effects in controlling the rate constant for hydride transfer,
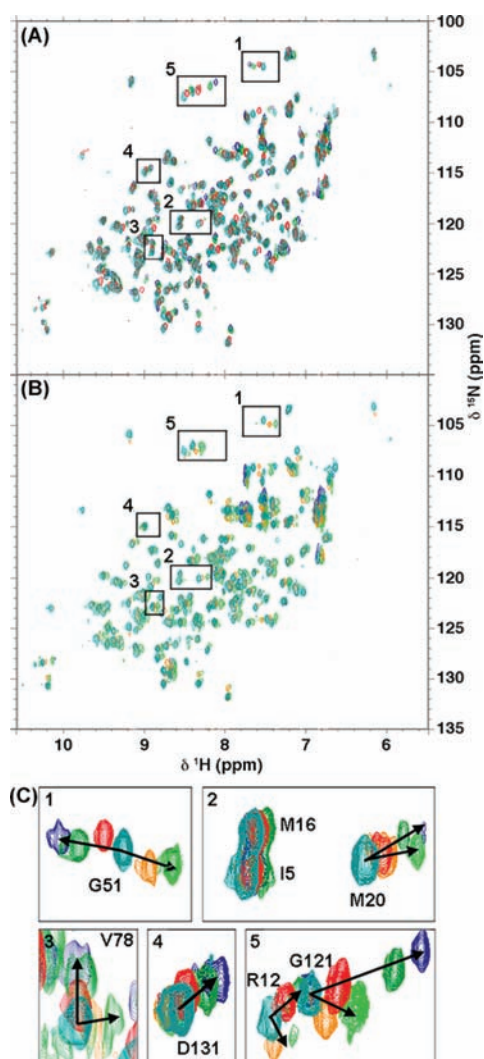
Figure 7. ^{1}H$-^{15}$N HSQC spectra of EcDHFR/NADP$^+$/folate in the presence of methanol (A) and glycerol (B). Insets (C) show expansions of certain regions of the spectra, demonstrating the different behavior of various peaks. Colors represent 0% (teal), 17% (red/orange), 33% (green/light green), and 50% (navy/blue) MeOH and glycerol. Spectra were acquired on 240 μM protein in 50 mM potassium phosphate buffer (pH 7.0) containing 1 mM NaCl, 10 mM β-mercaptoethanol, and 1.5 mM each NADP$^+$ and folate, on a Varian INOVA 600 MHz (^{1}H) spectrometer equipped with a 5 mm HCN probe.

while the absence of a viscosity effect rules out a direct coupling of large-scale motions to the actual hydride transfer step itself,[65,66] as increased viscosity would be expected to dampen such motions, and is hence not consistent with any model that invokes such long-range coupling. Computational studies including very recent work have highlighted the central role in EcDHFR catalysis of the electrostatic reorganization energy.[3,20] It is important to point out here that "large-scale" motions may be of small amplitude, but span a significant proportion of the protein. In addition, they may not be pure vibrational motions but may also include activated, diffusive motions uncoupled to vibrational modes. Our experimental results do not rule out shorter-range promoting motions that are uncoupled from the larger-scale motions of the protein but that could drive hydride transfer. Since such local motions are not slaved to the solvent,[66] the work described here does not

address their role in DHFR catalysis. While local motions may be protected from the effect of the solvent,[65,66] we consider it unlikely that a long-range motion could be protected in a similar way. Localized motions have been proposed to be important for hydride transfer in lactate dehydrogenase,[67] morphinone reductase,[65] and aromatic amine dehydrogenase.[10] For EcDHFR catalysis, it has been suggested that such promoting motions involve side chain rotation of Ile 14 and Ile 94,[68] residues that are conserved in MpDHFR.[26] However, if DHFR catalysis is dominated by electrostatic effects as our results and those of others[3,20] suggest, then there is no need to invoke such motions in catalysis. The alternative explanation for our results, that large-scale protein motions do couple to the chemical step but that changes to these motions do not manifest in the isotope effects or their temperature dependences, is unlikely since the KIE on hydride transfer is highly sensitive to changes to the donor–acceptor distance. A computational study of EcDHFR suggested that increasing the donor–acceptor distance from 3 to 3.5 Å led to an increase of the KIE by 60–100% at all temperatures; decreasing the temperature from 40 to 10 °C led to an increase in the KIE of only ∼10% when the donor–acceptor distance was held at 3 Å, or an increase of ∼40% when the donor–acceptor distance was maintained at 3.5 Å.[17] These results suggest that a change in the donor–acceptor distance as small as 0.05 Å would result in a change of 6–10% in the KIE, larger than a typical experimental error of stopped-flow measurements. The donor–acceptor distance in the NADP$^+$/folate complex of EcDHFR, a model of the ground-state Michaelis complex, is 3.3 Å,[53] requiring a decrease of 0.7 Å to meet the transition-state optimum.[69] Protein flexibility and motions may affect the rate constant for hydride transfer (k_H in MpDHFR is greater than in EcDHFR) as changes within the conformational ensemble will affect the electrostatic environment of the active site and therefore alter the barrier to the reaction, but do not affect the nature of the chemistry, as demonstrated by the very similar temperature dependences of the KIEs and the similar behavior in organic cosolvents. At the same time, NMR experiments show clear changes to EcDHFR in the presence of methanol and glycerol, despite little effect on the KIE. These results are in good agreement with our previous studies of EcDHFR,[13,36] which suggest that conformational changes influence the reaction, but through a more indirect route rather than through direct coupling. The conformational state of the enzyme at the time of hydride transfer may affect its rate constant, but no conformational change occurs during the hydride transfer event itself. The fact that mutations in the dimer interface of TmDHFR also cause the KIE to become entirely temperature independent across the whole temperature range (suggesting a long-range effect on a short-range motion,[12] while long-range motions are excluded by the kinetic results for TmDHFR obtained in the presence of cosolvents[14]) adds further support to the importance of prereaction conformational equilibria in DHFR catalysis.

The α-secondary hydrogen KIEs support an alternative view of the role of protein motions in DHFR catalysis. α-Secondary hydrogen KIEs at pH 7 have previously been reported for TmDHFR and the values obtained here are similar to those for the hyperthermophilic enzyme.[70] The temperature independent α-secondary KIEs observed for all three DHFRs, contrasting with the temperature dependent primary KIEs observed for MpDHFR and EcDHFR, support the suggestion that secondary KIEs report on events immediately prior to hydride transfer and/or are unaffected by the motions of the enzyme that affect the

20568

dx.doi.org/10.1021/ja208844j |*J. Am. Chem. Soc.* 2011, 133, 20561–20570

primary KIE.[70] Alternatively, our results might suggest that the temperature dependence of the KIE is in fact unaffected by protein motions altogether.

It has recently been suggested that our results with cosolvents are not relevant to dynamics coupled to hydride transfer,[6] as they relate to large-scale motions slaved to the solvent rather than internal protein motions slaved to the hydration shell.[66] However, the proposed network of coupled motions in DHFR is assumed to be involved in conformational changes, that is, those motions that are slaved to solvent, rather than coupled directly to hydride transfer.[6] Indeed, we have always been clear that our results do not comment on short-range internal protein motions that could potentially couple directly to hydride transfer (vide supra),[13,36] although changes to the solvent composition will most likely affect the hydration shell of the enzyme[71] and hence the internal protein motions slaved to it. Furthermore, others have suggested that the influence of viscosity on dynamics is felt even in the core of the protein.[72] Our results are fully consistent with a role for a network of coupled motions in DHFR that place the enzyme in an optimal conformation conducive to the reaction, the RRC, but not one directly coupled to hydride transfer itself. A recent NMR study connecting millisecond conformational fluctuations to hydride transfer[2] is not inconsistent with our results either as no claim of direct causality is made in that work. It is not surprising that conformational fluctuations influence the chemical step, as we have shown previously.[13,36] The central question is exactly how that influence is exerted, and how the chemistry is controlled within the RRC.

In summary, the results presented here provide strong evidence against a direct coupling of large-scale protein motions to the chemical step of the DHFR catalyzed reaction. They are consistent with previous studies that suggest that DHFR catalysis consists of a conformational search uncoupled from the chemistry itself, followed by hydride transfer, which may or may not involve short-range protein motions.[13,14,36] Protein flexibility may affect the rate of the reaction, presumably by altering the rate at which the RRC, an optimal conformation with the correct electrostatics and geometry for the reaction to occur, can be attained, but long-range motions do not directly couple to the reaction coordinate to change the nature of the chemistry itself.

Abbreviations. DHFR, dihydrofolate reductase; BsDHFR, DHFR from *G. stearothermophilus*; EcDHFR, DHFR from *E. coli*; MpDHFR, DHFR from *M. profunda*; TmDHFR, DHFR from *T. maritima*; NADP$^+$, nicotinamide adenine dinucleotide phosphate; NADPH, nicotinamide adenine dinucleotide phosphate (reduced form); KIE, kinetic isotope effect; CD, circular dichroism; HDX, hydrogen/deuterium exchange; HSQC, heteronuclear single quantum coherence; SOFAST-HMQC, band-selective optimized flip angle short transient heteronuclear multiple quantum coherence.

ASSOCIATED CONTENT

S **Supporting Information.** Circular dichroism spectra and melts; solvent dependence of k_{cat}/K_m; Kramers plot for k_H and k_{cat}; tabulated data for k_H, KIE(k_H), k_{cat}, KIE(k_{cat}), K_m and k_{cat}/K_m at 20 °C, and for the pH and temperature dependences of k_H and KIE(k_H); activation energies and Arrhenius prefactors; HDX data; NMR spectra. This material is available free of charge via the Internet at http://pubs.acs.org.

AUTHOR INFORMATION

Corresponding Author
AllemannRK@cf.ac.uk

Present Addresses
$^\|$Institute of Life Sciences, Swansea University, Singleton Park, Swansea, SA2 8PP, United Kingdom
$^\perp$Faculty of Science (Perak Campus), Universiti Tunku Abdul Rahman, Kampar, Perak, Malaysia
$^\#$Inorganic Chemistry Laboratory, University of Oxford, South Parks Road, Oxford, OX1 3QR, United Kingdom

REFERENCES

(1) Allemann, R. K.; Evans, R. M.; Loveridge, E. J. *Biochem. Soc. Trans.* **2009**, *37*, 349–353.

(2) Bhabha, G.; Lee, J.; Ekiert, D. C.; Gam, J.; Wilson, I. A.; Dyson, H. J.; Benkovic, S. J.; Wright, P. E. *Science* **2011**, *332* (6026), 234–238.

(3) Adamczyk, A. J.; Cao, J.; Kamerlin, S. C. L.; Warshel, A. *Proc. Natl. Acad. Sci. U.S.A.* **2011**, *108* (34), 14115–14120.

(4) Kamerlin, S. C. L.; Mavri, J.; Warshel, A. *FEBS Lett.* **2010**, *584* (13), 2759–2766.

(5) Pineda, J. R. E. T.; Antoniou, D.; Schwartz, S. D. *J. Phys. Chem. B* **2010**, *114* (48), 15985–15990.

(6) Nashine, V. C.; Hammes-Schiffer, S.; Benkovic, S. J. *Curr. Opin. Chem. Biol.* **2010**, *14* (5), 644–651.

(7) Nagel, Z. D.; Klinman, J. P. *Nat. Chem. Biol.* **2009**, *5* (8), 543–550.

(8) Henzler-Wildman, K.; Kern, D. *Nature* **2007**, *450* (7172), 964–972.

(9) Pudney, C. R.; Hay, S.; Levy, C.; Pang, J.; Sutcliffe, M. J.; Leys, D.; Scrutton, N. S. *J. Am. Chem. Soc.* **2009**, *131* (47), 17072–17073.

(10) Masgrau, L.; Roujeinikova, A.; Johannissen, L. O.; Hothi, P.; Basran, J.; Ranaghan, K. E.; Mulholland, A. J.; Sutcliffe, M. J.; Scrutton, N. S.; Leys, D. *Science* **2006**, *312* (5771), 237–241.

(11) Kuznetsov, A. M.; Ulstrup, J. *Can. J. Chem.* **1999**, *77* (5−6), 1085–1096.

(12) Loveridge, E. J.; Allemann, R. K. *Biochemistry* **2010**, *49* (25), 5390–5396.

(13) Loveridge, E. J.; Tey, L. H.; Allemann, R. K. *J. Am. Chem. Soc.* **2010**, *132* (3), 1137–1143.

(14) Loveridge, E. J.; Evans, R. M.; Allemann, R. K. *Chem.—Eur. J.* **2008**, *14* (34), 10782–10788.

(15) Swanwick, R. S.; Shrimpton, P. J.; Allemann, R. K. *Biochemistry* **2004**, *43* (14), 4119–4127.

(16) Zhang, Z. Q.; Rajagopalan, P. T. R.; Selzer, T.; Benkovic, S. J.; Hammes, G. G. *Proc. Natl. Acad. Sci. U.S.A.* **2004**, *101* (9), 2764–2769.

(17) Liu, H. B.; Warshel, A. *J. Phys. Chem. B* **2007**, *111* (27), 7852–7861.

(18) Pisliakov, A. V.; Cao, J.; Kamerlin, S. C. L.; Warshel, A. *Proc. Natl. Acad. Sci. U.S.A.* **2009**, *106* (41), 17359–17364.

(19) Hartsough, D. S.; Merz, K. M. *J. Am. Chem. Soc.* **1993**, *115* (15), 6529–6537.

(20) Liu, H. B.; Warshel, A. *Biochemistry* **2007**, *46* (20), 6011–6025.

20569

dx.doi.org/10.1021/ja208844j |*J. Am. Chem. Soc.* 2011, 133, 20561–20570

(21) Arai, M.; Iwakura, M.; Matthews, C. R.; Bilsel, O. *J. Mol. Biol.* **2011**, *410* (2), 329–342.

(22) Maglia, G.; Allemann, R. K. *J. Am. Chem. Soc.* **2003**, *125* (44), 13372–13373.

(23) Maglia, G.; Javed, M. H.; Allemann, R. K. *Biochem. J.* **2003**, *374*, 529–535.

(24) Loveridge, E. J.; Rodriguez, R. J.; Swanwick, R. S.; Allemann, R. K. *Biochemistry* **2009**, *48*, 5922–5933.

(25) Xu, Y.; Nogi, Y.; Kato, C.; Liang, Z.; Ruger, H.-J.; De Kegel, D.; Glansdorff, N. *Int. J. Syst. Evol. Microbiol.* **2003**, *53* (3), 533–538.

(26) Xu, Y.; Feller, G.; Gerday, C.; Glansdorff, N. *J. Bacteriol.* **2003**, *185*, 5519–5526.

(27) Hay, S.; Evans, R. M.; Levy, C.; Loveridge, E. J.; Wang, X.; Leys, D.; Allemann, R. K.; Scrutton, N. S. *ChemBioChem* **2009**, *10* (14), 2348–2353.

(28) Hata, K.; Kon, R.; Fujisawa, M.; Kitahara, R.; Kamatari, Y. O.; Akasaka, K.; Xu, Y. *Cell. Mol. Biol.* **2004**, *50* (4), 311–316.

(29) Evans, R. M.; Behiry, E. M.; Tey, L. H.; Guo, J. N.; Loveridge, E. J.; Allemann, R. K. *ChemBioChem* **2010**, *11* (14), 2010–2017.

(30) Murakami, C.; Ohmae, E.; Tate, S.; Gekko, K.; Nakasone, K.; Kato, C. *J. Biochem.* **2010**, *147* (4), 591–599.

(31) Murakami, C.; Ohmae, E.; Tate, S.; Gekko, K.; Nakasone, K.; Kato, C. *Extremophiles* **2011**, *15* (2), 165–175.

(32) Fierke, C. A.; Johnson, K. A.; Benkovic, S. J. *Biochemistry* **1987**, *26* (13), 4085–4092.

(33) Bieri, M.; Kwan, A. H.; Mobli, M.; King, G. F.; Mackay, J. P.; Gooley, P. R. *FEBS J.* **2011**, *278* (5), 704–715.

(34) Bai, Y. W.; Sosnick, T. R.; Mayne, L.; Englander, S. W. *Science* **1995**, *269* (5221), 192–197.

(35) Blakley, R. L. *Nature* **1960**, *188* (4746), 231–232.

(36) Loveridge, E. J.; Allemann, R. K. *ChemBioChem* **2011**, *12* (8), 1258–1262.

(37) Swanwick, R. S.; Maglia, G.; Tey, L.; Allemann, R. K. *Biochem. J.* **2006**, *394*, 259–265.

(38) Stone, S. R.; Morrison, J. F. *Biochemistry* **1982**, *21*, 3757–3765.

(39) Schanda, P.; Brutscher, B. *J. Am. Chem. Soc.* **2005**, *127* (22), 8014–8015.

(40) Delaglio, F.; Grzesiek, S.; Vuister, G. W.; Zhu, G.; Pfeifer, J.; Bax, A. *J. Biomol. NMR* **1995**, *6* (3), 277–293.

(41) Vranken, W. F.; Boucher, W.; Stevens, T. J.; Fogh, R. H.; Pajon, A.; Llinas, M.; Ulrich, E. L.; Markley, J. L.; Ionides, J.; Laue, E. D. *Proteins* **2005**, *59* (4), 687–96.

(42) Osborne, M. J.; Venkitakrishnan, R. P.; Dyson, H. J.; Wright, P. E. *Protein Sci.* **2003**, *12* (10), 2230–2238.

(43) Assignments for the MpDHFR/NADP+/folate complex have been deposited with the Biological Magnetic Resonance Data Bank (http://www.bmrb.wisc.edu/) under accession number BMRB 17946.

(44) Loveridge, E. J.; Behiry, E. M.; Swanwick, R. S.; Allemann, R. K. *J. Am. Chem. Soc.* **2009**, *131* (20), 6926–6927.

(45) Kramers, H. A. *Physica* **1940**, *7*, 284–304.

(46) Ansari, A.; Jones, C. M.; Henry, E. R.; Hofrichter, J.; Eaton, W. A. *Science* **1992**, *256* (5065), 1796–1798.

(47) Ivkovic-Jensen, M. M.; Kostic, N. M. *Biochemistry* **1997**, *36* (26), 8135–8144.

(48) Brouwer, A. C.; Kirsch, J. F. *Biochemistry* **1982**, *21* (6), 1302–1307.

(49) Goldberg, J. M.; Kirsch, J. F. *Biochemistry* **1996**, *35* (16), 5280–5291.

(50) Xu, Y.; Nogi, Y.; Kato, C.; Liang, Z. Y.; Ruger, H. J.; De Kegel, D.; Glansdorff, N. *Int. J. Syst. Evol. Microbiol.* **2003**, *53*, 533–538.

(51) Huber, R.; Langworthy, T. A.; Konig, H.; Thomm, M.; Woese, C. R.; Sleytr, U. B.; Stetter, K. O. *Arch. Microbiol.* **1986**, *144* (4), 324–333.

(52) Loveridge, E. J.; Maglia, G.; Allemann, R. K. *ChemBioChem* **2009**, *10* (16), 2624–2627.

(53) Sawaya, M. R.; Kraut, J. *Biochemistry* **1997**, *36* (3), 586–603.

(54) Osborne, M. J.; Schnell, J.; Benkovic, S. J.; Dyson, H. J.; Wright, P. E. *Biochemistry* **2001**, *40* (33), 9846–59.

(55) Venkitakrishnan, R. P.; Zaborowski, E.; McElheny, D.; Benkovic, S. J.; Dyson, H. J.; Wright, P. E. *Biochemistry* **2004**, *43* (51), 16046–16055.

(56) Yamamoto, T.; Izumi, S.; Gekko, K. *J. Biochem.* **2004**, *135* (1), 17–24.

(57) Yamamoto, T.; Izumi, S.; Gekko, K. *J. Biochem.* **2004**, *135* (6), 663–671.

(58) Polshakov, V. I.; Birdsall, B.; Feeney, J. *J. Mol. Biol.* **2006**, *356* (4), 886–903.

(59) McElheny, D.; Schnell, J. R.; Lansing, J. C.; Dyson, H. J.; Wright, P. E. *Proc. Natl. Acad. Sci. U.S.A.* **2005**, *102* (14), 5032–5037.

(60) Sham, Y. Y.; Ma, B. Y.; Tsai, C. J.; Nussinov, R. *Proteins* **2002**, *46* (3), 308–320.

(61) Meinhold, L.; Clement, D.; Tehei, M.; Daniel, R.; Finney, J. L.; Smith, J. C. *Biophys. J.* **2008**, *94* (12), 4812–4818.

(62) Agarwal, P. K.; Billeter, S. R.; Rajagopalan, P. T. R.; Benkovic, S. J.; Hammes-Schiffer, S. *Proc. Natl. Acad. Sci. U.S.A.* **2002**, *99* (5), 2794–2799.

(63) Oyeyemi, O. A.; Sours, K. M.; Lee, T.; Resing, K. A.; Ahn, N. G.; Klinman, J. P. *Proc. Natl. Acad. Sci. U.S.A.* **2010**, *107* (22), 10074–10079.

(64) Gunther, U. L.; Schaffhausen, B. *J. Biomol. NMR* **2002**, *22* (3), 201–209.

(65) Hay, S.; Pudney, C. R.; Sutcliffe, M. J.; Scrutton, N. S. *Angew. Chem., Int. Ed.* **2008**, *47* (3), 537–540.

(66) Frauenfelder, H.; Chen, G.; Berendzen, J.; Fenimore, P. W.; Jansson, H.; McMahon, B. H.; Stroe, I. R.; Swenson, J.; Young, R. D. *Proc. Natl. Acad. Sci. U.S.A.* **2009**, *106* (13), 5129–5134.

(67) Basner, J. E.; Schwartz, S. D. *J. Am. Chem. Soc.* **2005**, *127* (40), 13822–13831.

(68) Arora, K.; Brooks, C. L. *J. Am. Chem. Soc.* **2009**, *131* (15), 5642–5647.

(69) Wu, Y. D.; Houk, K. N. *J. Am. Chem. Soc.* **1987**, *109* (7), 2226–2227.

(70) Hay, S.; Pang, J. Y.; Monaghan, P. J.; Wang, X.; Evans, R. M.; Sutcliffe, M. J.; Allemann, R. K.; Scrutton, N. S. *ChemPhysChem* **2008**, *9* (11), 1536–1539.

(71) Micaelo, N. M.; Soares, C. M. *FEBS J.* **2007**, *274* (9), 2424–2436.

(72) Walser, R.; van Gunsteren, W. F. *Proteins* **2001**, *42* (3), 414–421.